Terminal Navigation Analysis for the 1980 Comet Encke Slow Flyby Mission

ROBERT A. JACOBSON,* JAMES P. MCDANELL,† AND GEORGE C. RINKER‡
Jet Propulsion Laboratory, Pasadena, Calif.

The initial results of a terminal navigation analysis for the proposed 1980 solar electric slow flyby mission to the comet Encke are presented. The navigation technique employs onboard optical measurements with the scientific television camera, ground-based observations of the spacecraft and comet, and ground-based orbit determination and thrust vector update computation. The knowledge and delivery accuracies of the spacecraft are evaluated as a function of the important parameters affecting the terminal navigation. These include optical measurement accuracy, thruster noise level, duration of the planned terminal coast period, comet ephemeris uncertainty, guidance initiation time, guidance update frequency, and optical data rate.

Introduction

At the present time there is considerable interest in the possible use of solar electric propulsion (SEP) for cometary exploration.[1-3] One of the leading candidates among the many possible missions is that of a slow flyby of the comet Encke during its 1980 apparition. The rationale for the selection of this mission from both a science and a mission planning standpoint is discussed in Refs. 1 and 4. Preliminary mission design studies[5] have defined a trajectory with a launch date of Dec. 17, 1978, and an arrival date of Nov. 6, 1980, with encounter occurring 30 days prior to Encke perihelion passage. The nominal encounter conditions for the preliminary trajectory, as dictated by the science requirements, consisted of a 20-day terminal coast with a closest approach of 3000 km at a relative velocity of 4 km/sec. The science requirements have since been revised,[4] and now impose a closest approach of 1000 ± 500 km, at a relative velocity of less than 5 km/sec, with a coast initiation no later than 6 days prior to encounter. The position and velocity constraints are necessary for successful operation of several of the onboard scientific instruments, and the terminal coast is needed to prevent contamination of the comet environment by the thruster exhaust.

In view of these new requirements, the preliminary design trajectory has been retargeted for an approach of 1000 km at 4 km/sec, with a 10-day terminal coast. Moreover, in order to more closely approximate an operational mission trajectory, piecewise constant clock angle, cone angle, and thrust magnitude controls were employed rather than a continuously varying optimal thrust vector control policy, and a variable specific impulse (2000–3000 sec, depending on power) was used rather than a constant specific impulse. The over-all heliocentric trajectory characteristics are shown in Fig. 1, and the mission parameters are summarized in Table 1.

The objective of this paper is to present a preliminary analysis of the terminal navigation problems associated with the execution of this nominal mission. It should be noted that a similar analysis was performed by Dazzo,[3] but with a somewhat different mission profile (i.e., no terminal coast) and a larger, more powerful spacecraft.

Table 1 1980 Encke slow flyby direct mission

Launch date	Dec. 17, 1978
Hyperbolic escape velocity	8.8 km/s
Time of flight	690 days
Mass launched	1170 kg
Solar power at 1 a.u.	8.5 kw
Arrival date	Nov. 6, 1980
Approach velocity	4 km/s
Delivered mass	800 kg
Solar distance at encounter	0.789 a.u.
Earth distance at encounter	0.330 a.u.

Terminal Navigation Assumptions

The terminal navigation phase of the mission begins at the time of acquisition of the comet with the onboard television camera.

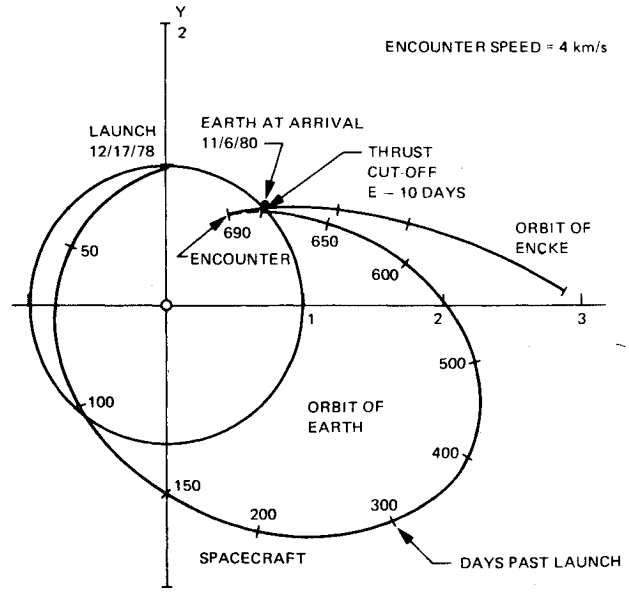

Fig. 1 1980 SEP Encke slow flyby.

Presented as Paper 73-1063 at the AIAA 10th Electric Propulsion Conference, Lake Tahoe, Nev., October 31–November 2, 1973; submitted November 29, 1973; revision received March 26, 1974. This paper presents one phase of research carried out at the Jet Propulsion Laboratory, California Institute of Technology, under NASA Contract NAS7-100.

Index categories: Navigation, Control, and Guidance Theory; Spacecraft Navigation, Guidance, and Flight-Path Control Systems.

* Senior Engineer, Mission Analysis Division. Associate Member AIAA.

† Member of Technical Staff, Mission Analysis Division.

‡ Engineer, Mission Analysis Division. Associate Member AIAA.

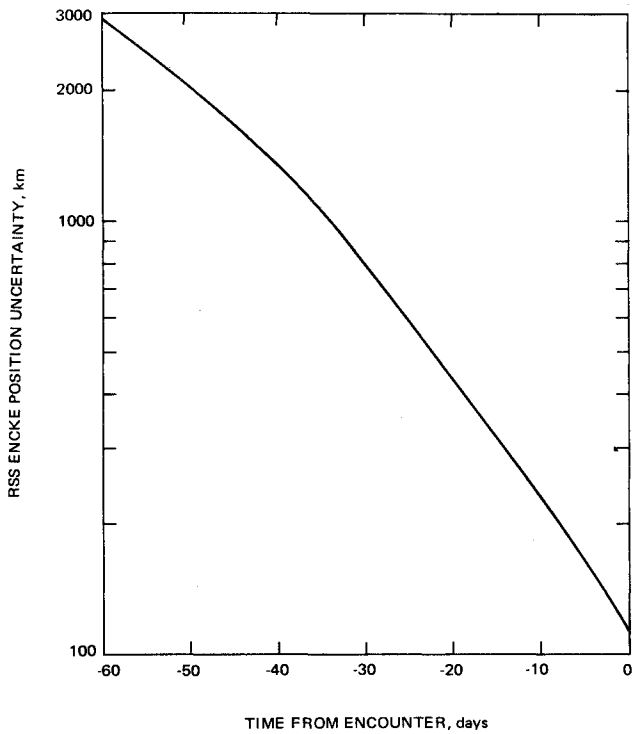

Fig. 2 Encke ephemeris improvement prediction.

For the baseline case this is assumed to occur 60 days prior to encounter at a distance of 28×10^6 km.

Error Sources and Observations

The comet-relative state errors at the beginning of the terminal navigation phase are dominated by the comet ephemeris uncertainty. The heliocentric state errors are assumed to be small compared with the ephemeris uncertainty at this time as a result of two-station radio tracking (QVLBI) for several days prior to the terminal navigation phase. The tracking stations at Goldstone and Madrid have favorably long overlapping view periods during this time period for ample two-station coverage. The effectiveness of this technique for precise heliocentric navigation of low thrust spacecraft is reported in Ref. 6.

Knowledge of the comet ephemeris is expected to improve with time as a result of Earth-based astronomical observations beginning in July of 1980, when the comet first becomes visible from Earth. The ephemeris improvement has been predicted by scientists at Goddard Space Flight Center,[7] and a time history of the expected uncertainty is given in Fig. 2.

Table 2 Baseline error source values

A priori state errors, 1σ	
Position	5000 km
Velocity	5 m/sec
Mass	20 kg
Thrust vector biases, 1σ	
Magnitude	(Equivalent to mass state error)
Direction	10 mrad
Thrust vector noise	
Magnitude	
Standard deviation	2% of nominal thrust
Correlation time	2 days
Direction	
Standard deviation	10 mrad
Correlation time	2 days

Table 3 Mariner Mars 1971 imaging experiment characteristics

Characteristic	Camera B
Effective focal length	500 mm
Focal ratio	f/2.35
T-number	T/4.0
Approximate fastest shutter speed	3 msec
Angular field-of-view (diagonal)	1.8 deg
Active target raster	9.6×12.5 mm
Aspect ratio	1.30:1
Active scan lines per frame	700
Frame time	42 sec
Total line time	60 msec
Active line time	56.6 msec
Line sync time	3.4 msec
Approximate black mask time	1.0 msec
Active picture elements per line	832
Bits/picture element	9
Video carrier frequency	28.8 kHz
Video baseband	7,35 kHz
Video sampling frequency	14.7 kHz
Video passband	21.45–36.15 kHz
Resolution at 1800 km	0.1 km/pixel pair
Number of filters	1
Weight (platform)	14 kg
Size	$81 \times 25 \times 25$ cm

Other error sources include thrust vector biases, caused by off-nominal performance of the thruster and its supporting subsystems, and random accelerations (process noise) due to stochastic temporal variations in the thrust vector magnitude and direction. The latter represents a continuous source of trajectory disturbance during the powered portion of the terminal phase. The baseline assumptions for the comet-relative a priori state errors, thrust vector biases, and thruster noise are summarized in Table 2. The thrust vector biases and noise model standard deviations were selected in accordance with expected attitude control tolerances and the SEP thrust subsystem statistical error model of Ref. 8. The correlation times were selected to give conservative terminal state error statistics, as will be shown in a later section.

The primary source of data for terminal navigation is the onboard science television camera. The Mariner Mars 1971 B camera (narrow angle) has been tentatively selected to satisfy science requirements; consequently, this camera was assumed for the baseline navigation analysis. Its characteristics are given in Table 3.

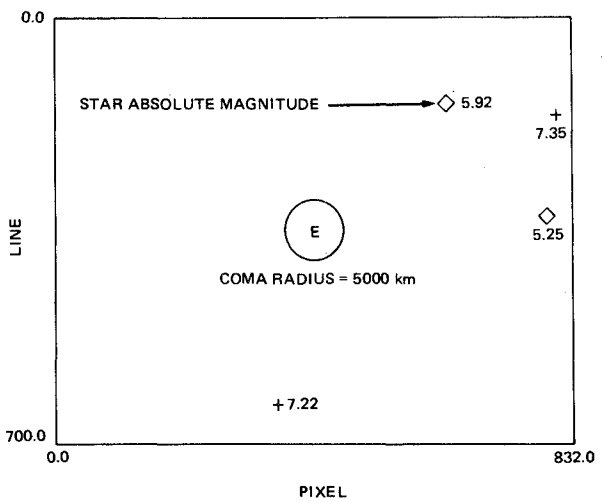

Fig. 3 TV image of comet Encke and star background at 10 days before encounter.

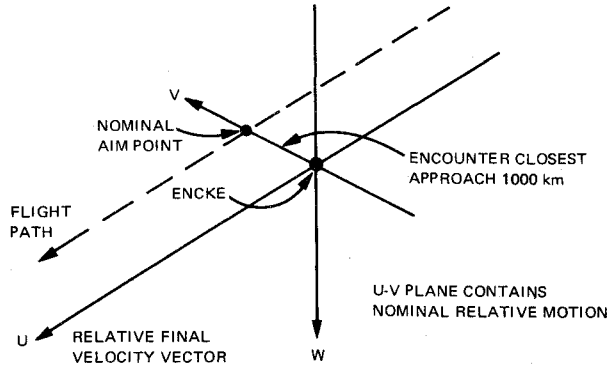

Fig. 4 Impact plane system.

For navigation purposes, the comet must be imaged against a star background. The onboard camera is capable of resolving images brighter than 9th magnitude, and the current mission profile guarantees at least three stars of sufficient brightness in the picture at all times. An example of a simulated picture 10 days before encounter is given in Fig. 3; the comet image represents a view of the inner coma, which is assumed to be 5000 km in radius. The currently predicted outer coma of 50,000 km would fill the screen at this time; however, the outer coma is believed to be sufficiently diffuse to permit stars to be imaged through it.

It is assumed that the comet nucleus coincides with the center of brightness and that the center of brightness can be resolved to a single picture element (pixel). This corresponds to an angular resolution of approximately 30μ rad for the optical observations.

Although the television camera provides effective comet-relative position information normal to the local line-of-sight, it provides no instantaneous target-range information. Furthermore, since the line-of-sight direction rotates very little during the powered portion of the terminal phase, there is little transfer of cross-range information into the down-range direction. The target-range information must, therefore, be inferred from Earth-based observations and consequently is limited by the ephemeris uncertainty.

Since the Earth-based data types (both spacecraft and comet observations) are needed to supplement the onboard optical data only for the purpose of inferring target-range, their effect can be adequately represented as a direct target-range measurement weighted so that the down-range error follows the ephemeris uncertainty curve of Fig. 2. This is the approach used for the present study. The measurement schedules and accuracies are given in Table 4.

Orbit Determination and Trajectory Correction

The orbit determination filter employed in the analysis was a discrete form of the Kalman sequential filter.[9,10] The random thrust errors (process noise) were treated as piecewise constant functions over one hour time intervals, closely approximating a continuous first-order Gauss-Markov process.

The trajectory correction algorithm was a discrete linear optimal guidance strategy[11] which minimizes expected terminal position errors by computing variations in the encounter time and piecewise constant updates to the nominal thrust vector control policy. The characteristics of the trajectory update policy, including the length of the time interval over which control corrections are constant, the cycle time (i.e., update rate), and the limits on the size of the corrections are given in Table 5. The guidance cycle was selected to be representative of one which might be implemented in actual operations. The control constraints reflect hardware and power limitations of the spacecraft.

Table 4 Baseline observation schedule

Measurement type	Data rate	Accuracy (1σ)
TV pictures	4 pictures/day	1 pixel
Relative range	1 point/day	Follows comet ephemeris (Fig. 2)

Table 5 Baseline trajectory update strategy

Control variables	Interval of constant control	Guidance cycle	Control constraints (1σ)
Clock and cone angles	2 days	2 days	± 0.1 radians
Thrust magnitude	2 days	2 days	$\pm 5.0\%$ of nominal thrust

Baseline Navigation Analysis

The navigation system must accomplish the following two objectives:

Delivery: With a combination of orbit determination and trajectory corrections, deliver the spacecraft to the desired encounter conditions.

Knowledge: After the last trajectory correction has been performed, but before the encounter science sequence is commanded, determine the achieved trajectory.

For the analysis in this paper the measure of delivery accuracy will be the semimajor axis of the 1σ position error ellipse in the impact plane (plane normal to the relative velocity vector at encounter, Fig. 4). Errors in this plane must be removed using corrections to the nominal thrust vector control program, but errors normal to it may be eliminated by a time-of-flight correction. Since, for the baseline mission profile, the last trajectory correction must of necessity terminate at coast initiation 10 days prior to encounter, and the science sequence begins shortly thereafter, the measure of knowledge accuracy will be the orbit determination error at that time mapped to the impact plane at encounter. This measure of knowledge also represents the theoretical limiting delivery accuracy. As in the case of delivery, the quantitative measure of knowledge will be the semimajor axis of the 1σ error ellipse.

The 1σ delivery and knowledge error ellipses in the impact plane for the baseline case are displayed in Fig. 5. These ellipses, which have semimajor axes of 1568 and 689 km, respectively, show the failure of the baseline navigation system to achieve the specified accuracy of ± 500 km.

In order to understand the reason for the large knowledge error, a breakdown of the contributions of the various error sources is given in Fig. 6. It is clear that the errors are dominated by the effect of the process noise, closely followed by the data noise, and that the ephemeris uncertainty and the biases are of

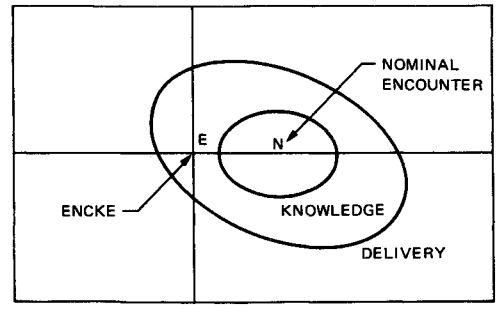

Fig. 5 1σ knowledge and delivery ellipses in impact plane at encounter.

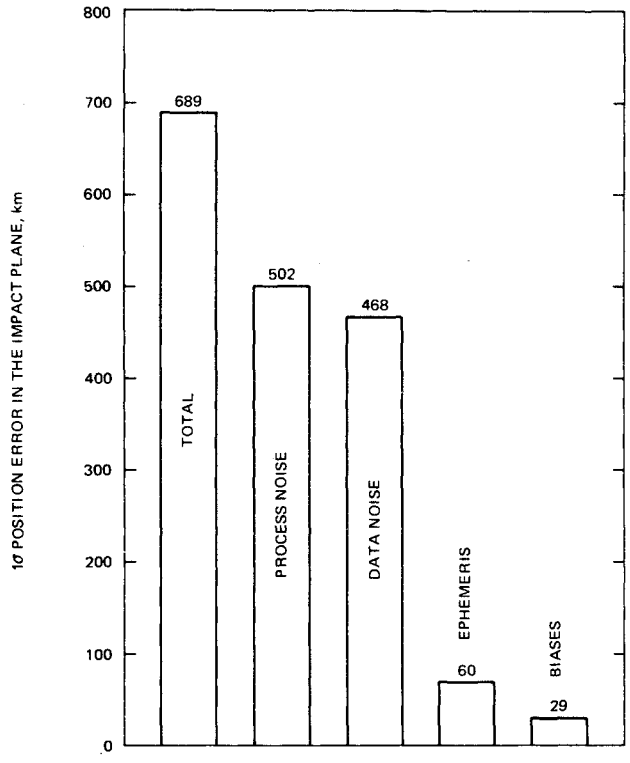

Fig. 6 Relative contribution of the various orbit determination error sources to the total knowledge error in the impact plane.

minor importance. The total error is the rss of the individual components.

The magnitude of the delivery error relative to the knowledge error suggests that some improvement in the guidance law is possible. However, the knowledge error of Fig. 5 represents ultimate delivery accuracy only if infinite control effort can be applied just prior to engine shutdown (i.e., an impulsive maneuver). The actual delivery accuracy, as shown by Fig. 7, is limited by the knowledge error at the last guidance update time mapped to encounter and including the effect of the process noise during the last guidance cycle. As indicated by the figure, the guidance law does in fact attain the limiting delivery accuracy; and therefore, is "perfect" in the sense that all known errors are accounted for.

A time history of the position and velocity knowledge errors in the viewing plane (plane normal to the instantaneous line-of-sight, Fig. 8) is presented in Fig. 9. Error reductions in this plane are due to the onboard optical measurements which provide information normal to the line-of-sight, rather than

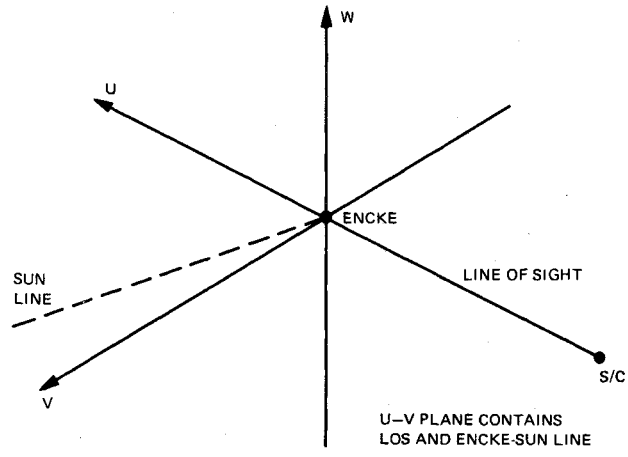

Fig. 8 Viewing plane system.

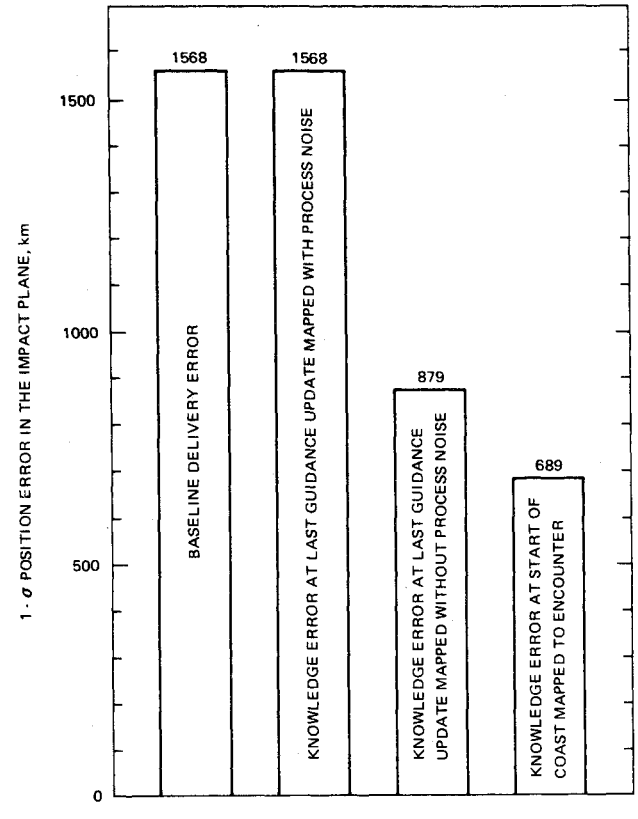

Fig. 7 Relative contribution of knowledge error and process noise to delivery error.

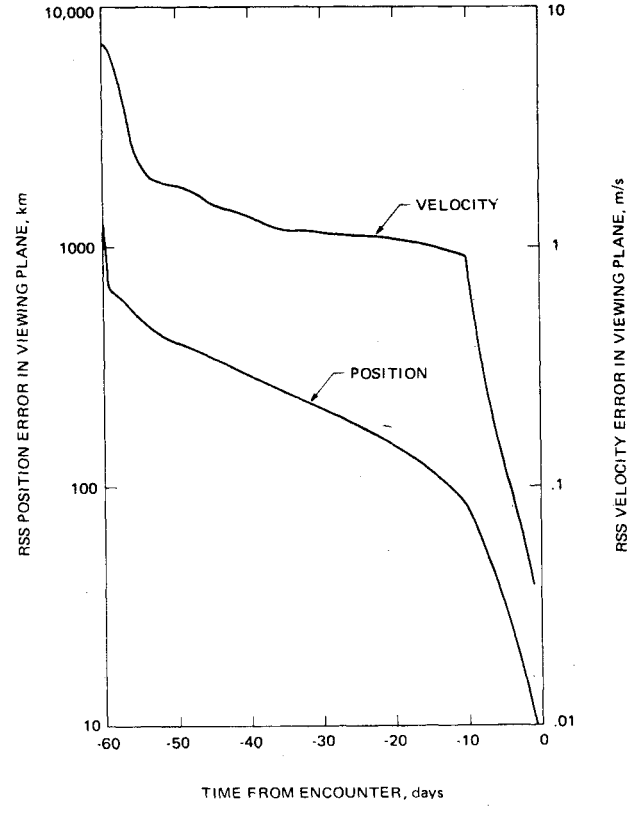

Fig. 9 Time history of baseline knowledge errors.

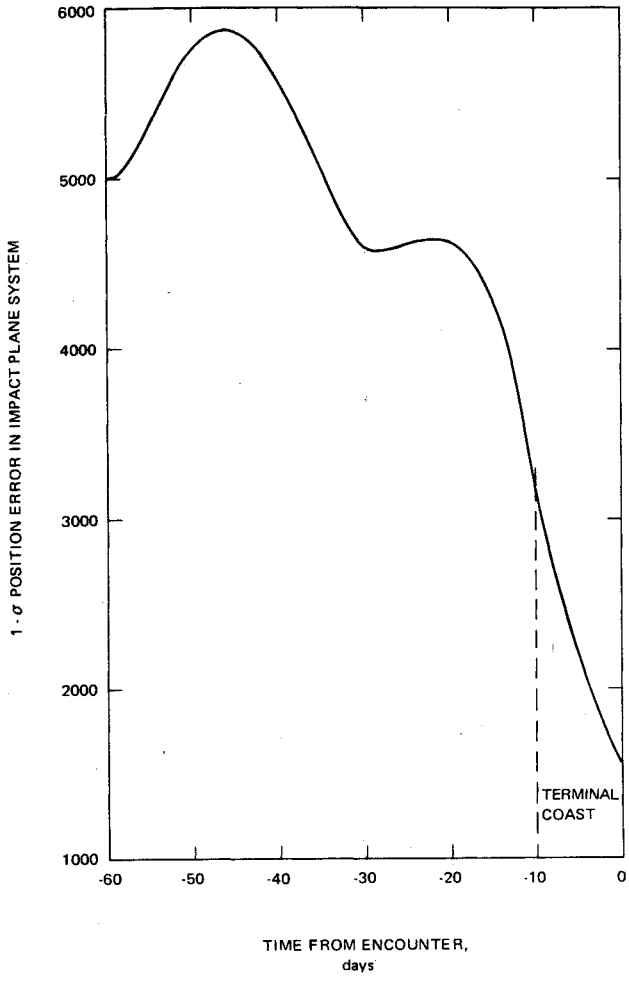

Fig. 10 Time history of baseline delivery errors.

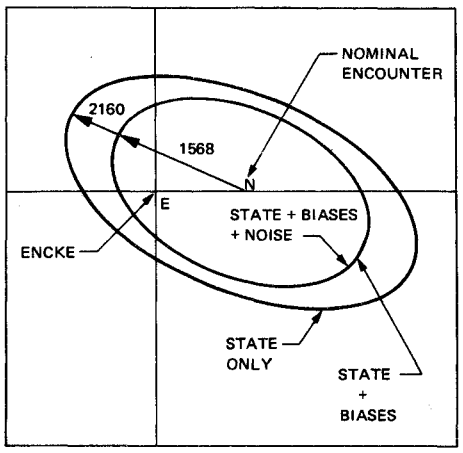

Fig. 12 1σ delivery ellipses as a function of guidance strategy.

because of the inferred range which gives information along the line-of-sight. Although the errors decrease continuously during the navigation period, they remain at an unacceptable level until the coast is entered and the process noise is removed as an error source. One of the major limiting factors in the terminal navigation is the inability of the optical data to provide adequate velocity information in the presence of the process noise. Note from the figure that the velocity cannot be determined to better than about 1 m/sec until the engines are shut down. This large velocity uncertainty contributes significantly to the mapped knowledge error which, in turn, limits delivery accuracy.

A time history of the position delivery error in the impact plane is given in Fig. 10. Errors in this plane are corrected using the angle and throttle controls, while errors normal to it (i.e., along the final relative velocity vector) can be corrected by a variation in time-of-flight. For the baseline case the standard deviation of the time of flight variation is 7.375 hours. Figure 11 shows the standard deviations of the thrust magnitude and cone angle corrections commanded by the guidance algorithm (clock angle corrections are similar to those of the cone angle). It is clear from these figures that guidance activity occurs in two phases. First the a priori state errors are removed to the extent that knowledge permits; then the errors introduced by the process noise and those found as a consequence of improved knowledge are corrected.

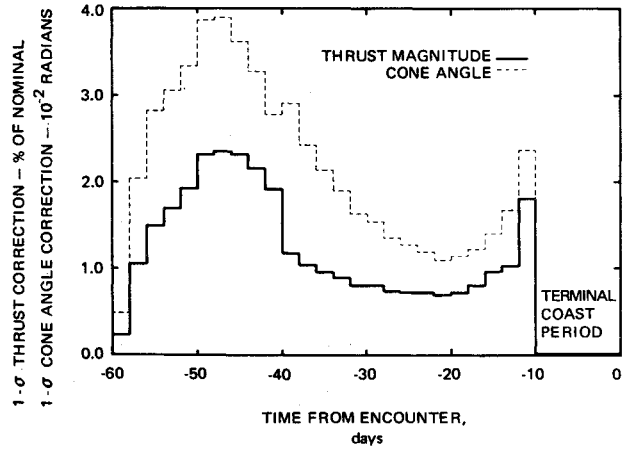

Fig. 11 Baseline thrust vector guidance corrections.

Parameter Studies

Variations in Guidance Strategy

The guidance algorithm normally bases its control corrections on estimates of the spacecraft state, the bias parameters, and the parameters in the process noise model. The impact plane delivery error ellipses in Fig. 12 show the loss of effectiveness when the process noise or the process noise and the biases are neglected in the guidance law. The 25 km error increase caused by ignoring the process noise cannot be seen in the figure, but the 592 km increase when both the noise and the biases are ignored is readily apparent.

The baseline guidance strategy employed a cycle of two days and required engine throttling. Table 6 gives the impact plane delivery errors which result when more frequent (daily) updates are used, and when control is restricted to cone and clock angles only. The elimination of engine throttling has no effect on delivery accuracy, but causes an increase in the time-of-flight standard deviation of about 2 hr. The daily update strategy leads to an improvement of about 452 km. This primarily is because

Table 6 Alternative guidance strategy results

Guidance procedure	Final position 1σ error	Encounter time standard deviation	Maximum throttle standard deviation
Nominal	1567.9 km	7.375 hr	2.35%
Angles only	1567.9 km	9.394 hr	0.00%
Daily updates	1115.8 km	7.423 hr	4.30%

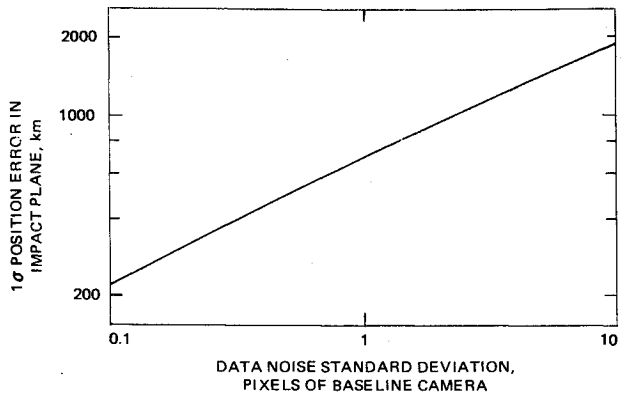

Fig. 13 Knowledge errors as a function of optical data noise.

only one day of process noise corrupts the trajectory between the last update and the start of the final coast.

Data Noise and Ephemeris Errors

If difficulty arises in identifying the comet's center of brightness, or failure to image stars through the coma forces camera pointing to be performed relative to an onboard inertial platform, larger data noise than the baseline of one pixel will occur. On the other hand, if a higher resolution camera is used, optical measurement errors can be reduced. The effect of variations in optical data noise level on the position knowledge error is shown in Fig. 13. Clearly, the navigation process is very sensitive to the resolution of the optical measurements.

Since the uncertainty in the relative range corresponds directly to that of the ephemeris, any changes in the predicted ephemeris uncertainty will ostensibly have an effect on the knowledge error. However, it was found that knowledge error in the impact plane is only a very weak function of the ephemeris uncertainty. Indeed, an order of magnitude increase in ephemeris uncertainty increases the knowledge error in the impact plane by less than 1%.

Variations in Navigation Start Time

Delaying the start of terminal navigation forces trajectory corrections to be made in a shorter period of time and also increases knowledge errors because fewer onboard optical measurements can be made. However, as seen in Fig. 14, sizable delays are possible with little degradation in knowledge and delivery accuracy, but delays of more than 30 days result in rapidly increasing delivery errors as the controllability limit of the spacecraft is approached.

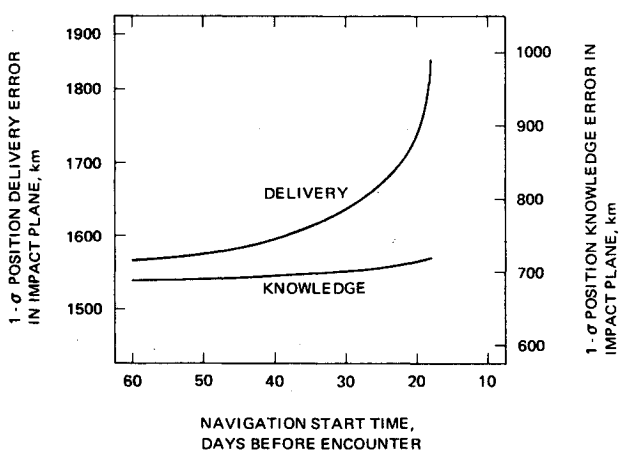

Fig. 14 Final knowledge and delivery errors as a function of navigation start time.

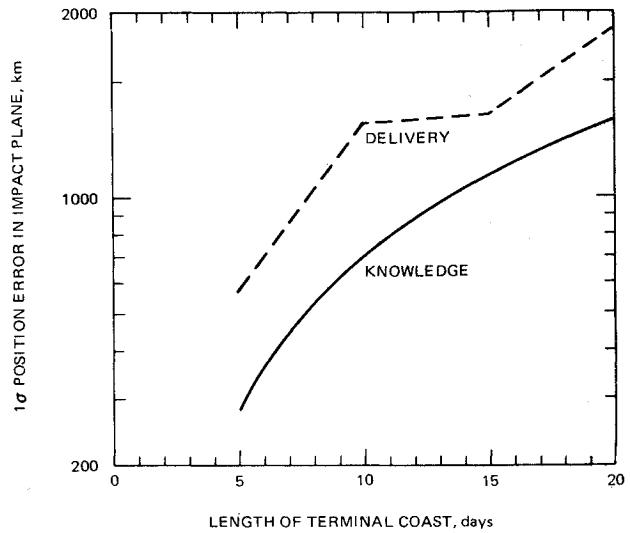

Fig. 15 Final knowledge and delivery error as a function of coast duration.

Variations in Duration of Final Coast

The baseline mission terminal coast forces all trajectory correction to cease 10 days prior to nominal encounter. Consequently, any errors remaining at that time map into the final delivery errors. If the coast is shortened, smaller delivery errors result because a longer period for orbit determination and guidance is available, and because errors remaining at the start of the coast are mapped over a shorter time interval. Conversely, if the coast is lengthened, larger delivery errors occur due to the shorter guidance period and the longer mapping time. Figure 15 gives the impact plane knowledge and delivery errors for various coast lengths. The delivery error is not a smooth function because the last guidance cycle contains one day of uncorrected process noise when the coast has an odd number of days, but contains two days of uncorrected noise when the coast has an even number of days. It is clear from the figure that shorter coast lengths can lead to a significant improvement in final position error.

Process Noise Levels

As indicated by Fig. 6, process noise is one of the dominant error sources, and if it is reduced, significant improvement in final errors can be expected. The relation between noise level and final knowledge and delivery accuracy is shown by Fig. 16.

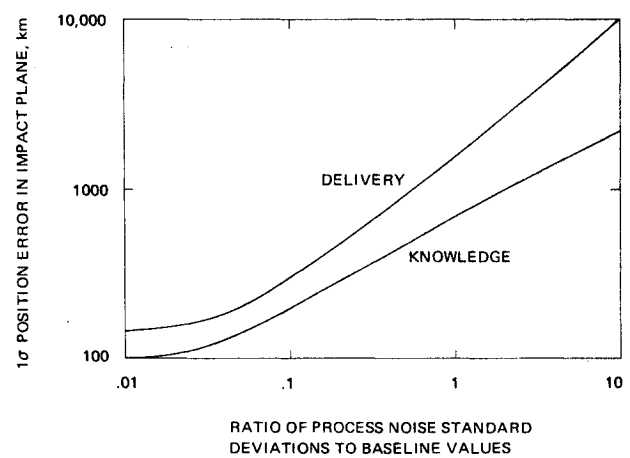

Fig. 16 Final knowledge and delivery errors as a function of process noise.

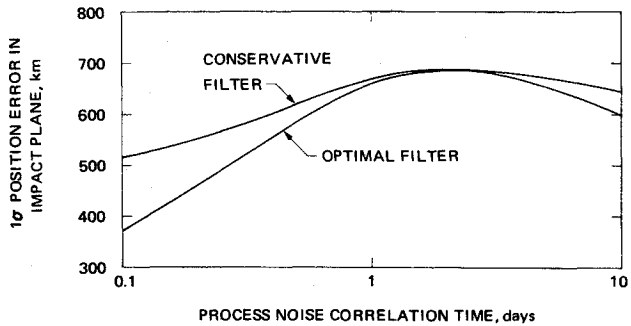

Fig. 17 Terminal knowledge error as a function of correlation time.

After the noise level is reduced by an order of magnitude, the improvement rate slows because the noise has ceased to dominate the other errors. When the noise is increased, the knowledge and delivery curves diverge because of the effect of the uncorrected noise in the last guidance cycle (see Fig. 7).

Correlation Times

The correlation times for the thrust error model are somewhat nebulous and more difficult to determine from physical data than the standard deviations. Observed time variations of quantities contributing to the thrust magnitude error tend to suggest correlations on the order of days, whereas pointing errors appear to vary more rapidly. To simplify the navigation analysis the same correlation time was assumed for thrust pointing errors as for the thrust magnitude error. However, it can be seen from Fig. 17 that the baseline value of two days is a conservative choice, as this value corresponds to the maximum knowledge error as a function of correlation time. The parametric analysis with respect to correlation time was done two ways. The curve labeled "optimal filter" in Fig. 17 gives the error when the filter model correlation time matches that of the actual process noise. The other curve represents the performance as a function of the actual correlation time when the filter model correlation time remains fixed at the baseline value of two days. Clearly, the navigation process in this case is not vulnerable to correlation time mismatch, as the realized performance in each case is better than the indicated baseline performance.

Optical Data Rate

Because of the process noise, knowledge degrades rapidly between orbit determination updates, i.e., data points. In order to assess the effect of a higher data rate on slowing the degradation, a data rate of one picture per hour was investigated. An improvement of about 200 km was obtained in the final knowledge accuracy, and an improvement of about 225 km occurred in the final delivery accuracy.

Conclusions

The baseline mission and navigation system design as defined in this paper cannot achieve the desired delivery accuracy of 500 km for the proposed Encke slow flyby. The basic source of difficulty is the inability of the optical data to adequately determine the velocity in the presence of high level process noise.

The parametric analysis suggests some potential means for improving terminal navigation. First, the nominal mission can be redesigned for the shortest terminal coast possible without compromising scientific objectives. Shortening the terminal coast from 10 to 6 days would improve delivery accuracy by almost a factor of two. Making guidance corrections more frequently near the time of thrust cutoff, and taking more data are other means for achieving substantial improvement without major changes to the basic navigation strategy or system hardware. A higher resolution optical sensor could also be implemented if necessary; however, it is more cost effective to use the science TV camera for navigation if possible. Another approach which remains to be investigated is the possible use of one or more short ballistic coast arcs prior to the final coast period to obtain more precise orbit determination as the basis for the final trajectory corrections.

References

[1] Atkins, K. L. and Moore, J. W., "Cometary Exploration: A Case for Encke," *Journal of Spacecraft and Rockets,* to be published.

[2] Meissinger, H. F., Greenstadt, E., Axford, I., and Wetherill, G., "Comet Exploration: Scientific Objectives and Mission Strategy for a Rendezvous with Comet Encke," AIAA Paper 73-550, Denver, Colo., 1973.

[3] Dazzo, E. J., "Solar Electric Low Thrust Performance Capability for an Early Flyby Mission to Comet Encke," presented at the AAS/AIAA Astrodynamics Conference, Vail, Colo., 1973.

[4] Newburn, R. L. et al., "Science Rationale and Instrument Package for a Slow Flyby of Comet Encke," Doc. 760-90, June 1, 1973, Jet Propulsion Lab., Pasadena, Calif.

[5] Bender, D. F., Atkins, K. L., and Sauer, C. G., "Mission Design for a 1980 Encke Slow Flyby Using Solar Electric Propulsion," presented at the AAS/AIAA Astrodynamics Conference, Vail, Colo., 1973.

[6] McDanell, J. P., "Earth Based Orbit Determination for Solar Electric Spacecraft with Application to a Comet Encke Rendezvous," AIAA Paper 73-174, Washington, D.C., 1973.

[7] Farquhar, R. W., private communication, July, 1973, NASA Goddard Space Flight Center, Greenbelt, Md.

[8] Bantell, M. H., "Statistical Error Model for a Solar Electric Propulsion Thrust Subsystem," TM 33-607, June 1, 1973, Jet Propulsion Lab., Pasadena, Calif.

[9] Bryson, A. E. and Ho, Y. C., *Applied Optimal Control,* Blaisdell, Waltham, Mass., 1969.

[10] Kalman, R. E., "New Methods and Results in Linear Prediction and Filtering Theory," TR 61-1, 1961, Research Institute for Advanced Studies, Martin Marietta Corp., Baltimore, Md.

[11] Jacobson, R. A., "A Constrained Discrete Optimal Guidance Strategy for Low Thrust Spaceflight," presented at the AAS/AIAA Astrodynamics Conference, Vail, Colo., 1973.